The EMBO Journal Vol.18 No.12 pp.3317–3324, 1999

Extracellular links in Kir subunits control the unitary conductance of SUR/Kir6.0 ion channels

Vez P.Repunte, Haruki Nakamura[1], Akikazu Fujita, Yoshiyuki Horio, Ian Findlay[2], Lutz Pott[3] and Yoshihisa Kurachi[4]

Department of Pharmacology II, Faculty of Medicine and Graduate School of Medicine, Osaka University, 2-2 Yamada-oka, Suita, Osaka 565-0871, Japan, [1]Department of Bioinformatics, BERI, 6-2-3 Furuedai, Suita, Osaka 565-0874, Japan, [2]CNRS UMR 6542, Faculté des Sciences, Université de Tours, Tours F-37200, France and [3]Department of Physiology, Ruhr University Bochum, D-44780 Bochum, Germany

[4]Corresponding author
e-mail: ykurachi@pharma2.med.osaka-u.ac.jp

Potassium (K^+) channels are highly selective for K^+ ions but their unitary conductances are quite divergent. Although Kir6.1 and Kir6.2 are highly homologous and both form functional K^+ channels with sulfonylurea receptors, their unitary conductances measured with 150 mM extracellular K^+ are ~35 and 80 pS, respectively. We found that a chain of three amino acid residues N123–V124–R125 of Kir6.1 and S113–I114–H115 of Kir6.2 in the M1–H5 extracellular link and single residues M148 of Kir6.1 and V138 of Kir6.2 in the H5–M2 link accounted for the difference. By using a 3D structure model of Kir6.2, we were able to recognize two independent plausible mechanisms involved in the determination of single channel conductance of the Kir6.0 subunits: (i) steric effects at Kir6.2V138 or Kir6.1M148 in the H5–M2 link influence directly the diffusion of K^+ ions; and (ii) structural constraints between Kir6.2S113 or Kir6.1N123 in the M1–H5 link and Kir6.2R136 or Kir6.1R146 near the H5 region control the conformation of the permeation pathway. These mechanisms represent a novel and possibly general aspect of the control of ion channel permeability.

Keywords: chimera/conductance/inwardly rectifying K^+ channel/Kir6.0 subunit/structure

Introduction

Potassium (K^+) channels are highly selective to K^+ ions. Recent structural analysis of the pore region of a bacterial K^+ channel (KcsA) has revealed how a K^+ channel can be more selective for K^+ than smaller cations such as sodium and lithium, yet possess high unitary conductance (Doyle *et al.*, 1998). However, the unitary conductance of different K^+ channels is quite divergent and ranges from femtoSiemens to hundreds of picoSiemens (Butler *et al.*, 1993; Krapivinsky *et al.*, 1998), which indicates that structural elements other than the pore-forming region are involved in the control of permeation properties of K^+ channels.

In gross terms, the mammalian equivalent of the bacterial KcsA channel is the inwardly rectifying K^+ (Kir) channels (Jan and Jan, 1997) whose subunit possesses a simple structure of intracellular C- and N-termini, two transmembrane-spanning regions (M1 and M2) and an extracellular loop which contains the pore-forming H5 region. Kir6.1 and Kir6.2 belong to the same subfamily of Kir subunits and are highly homologous with ~70% identity in the primary amino acid sequence. Both form functional K^+ channels when expressed with sulfonylurea receptors (SURs) (Inagaki *et al.*, 1995a, 1996; Sakura *et al.*, 1995; Isomoto *et al.*, 1996; Yamada *et al.*, 1997; Satoh *et al.*, 1998). These functional K^+ channels are conceived to have an octameric or tetradimeric structure with a $(Kir6.0/SUR)_4$ stoichiometry (Clement *et al.*, 1997; Shyng and Nichols, 1997) whose conductance properties are determined by the pore-forming Kir6.0 subunits. Of particular interest to us here is the fact that the unitary conductance of the Kir6.1/SUR channel is ~35 pS while that of the Kir6.2/SUR channel is ~80 pS (Inagaki *et al.*, 1995a, 1996; Isomoto *et al.*, 1996; Yamada *et al.*, 1997; Kondo *et al.*, 1998). The amino acid sequences of the pore-forming H5 regions of Kir6.1 and Kir6.2 are identical, which led us to speculate that the major determinants for the unitary conductance of Kir6.0 channels should reside outside the H5 region.

Here we show that the extracellular loops which link the transmembrane-spanning domains and the H5 pore region control the permeability of Kir6.0/SUR channels. A group of three amino acid residues in the M1–H5 link, N123–V124–R125 of Kir6.1 and S113–I114–H115 of Kir6.2, and a single amino acid residue in the H5–M2 link, M148 of Kir6.1 and V138 of Kir6.2, are responsible for the different single channel conductances of Kir6.1/SUR and Kir6.2/SUR channels. A tertiary model of the Kir6.2 channel revealed that while the amino acid residue in the H5–M2 link might directly influence ion passage through the channel pore, the three amino acid residues in the M1–H5 link were more likely to be involved in determining the conformation of the permeation pathway. This represents a novel and possibly general aspect of the control of ion channel permeability.

Results

Structural determinants of the single channel conductance of SUR2A/Kir6.0 K^+ channels

Although we have previously shown that the SUR subunit has no influence upon single channel conductance of Kir/SUR channels, in this study we expressed the different Kir6.0 subunits and subsequently their chimeras, with a single type of SUR, SUR2A. Attention also focused upon

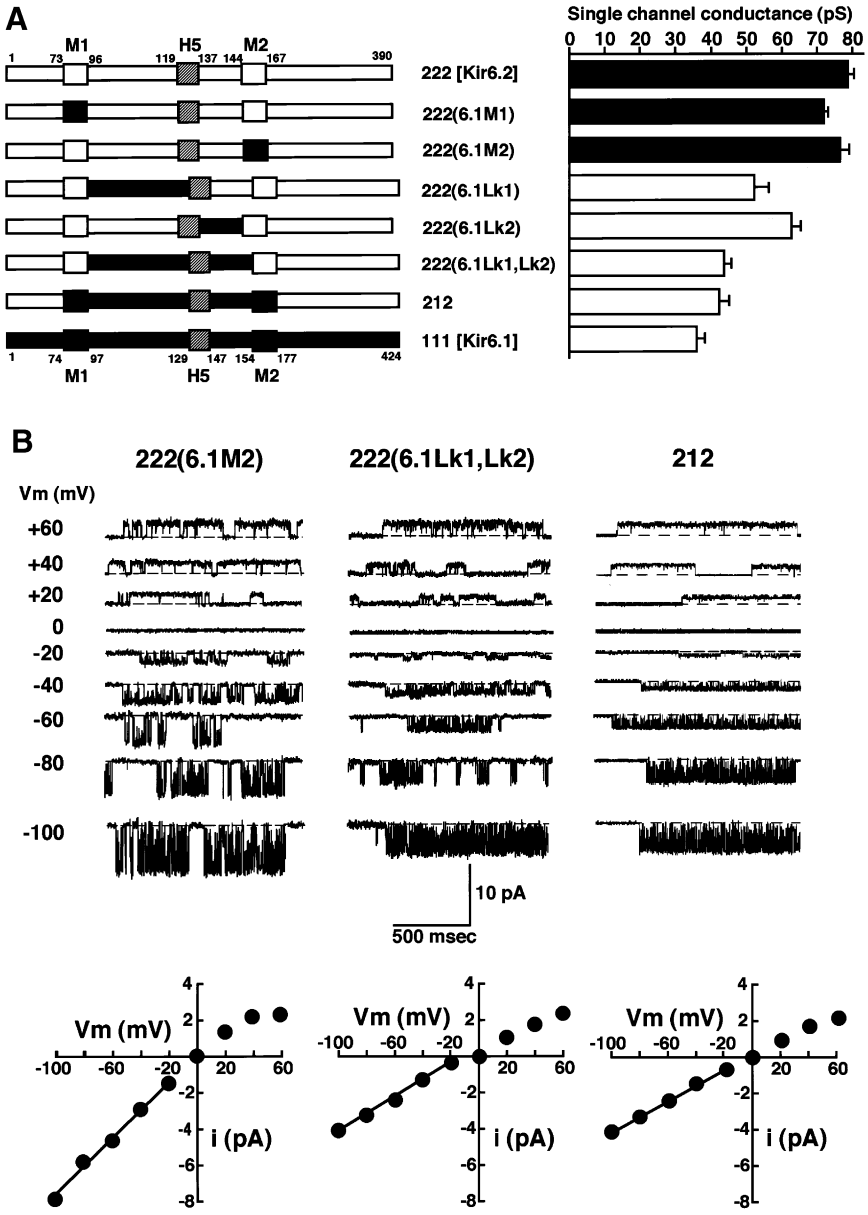

Fig. 1. Influence of the extracellular links and transmembrane domains on the unitary conductances of Kir6.0/SUR2A channels. (**A**) Schematic diagram of wild-type and chimeric constructs of Kir 6.0 subunits (left panel) and their respective average unitary conductances (right panel). Nomenclature is as follows: 111, wild-type Kir6.1; 222, wild-type Kir6.2. The three numbers represent the C-terminus, the core region (M1–H5–M2) and the N-terminus, respectively. We divided the core region of Kir6.0 subunits into five parts; M1, Lk1, H5, Lk2 and M2, and constructed a variety of chimeras based upon Kir6.2 with segments replaced by the corresponding section of Kir6.1. The numbering refers to the amino acid boundaries of each domain. Kir6.1 domains are shaded and the H5 region which is common to Kir6.1 and Kir6.2 is hatched. The mean ±SD value of single channel conductance obtained from four or five different patches for each chimera is presented in the right panel. (**B**) Single channel currents recorded at different membrane potentials (shown in the upper section of each panel) and the relation between unitary channel current amplitude and membrane potential (shown in the lower section) of representative chimeras. Left panel, the 222(6.1M2)/SUR2A channel. Middle panel, the 222(6.1Lk1,Lk2)/SUR2A channel. Right panel, the 212/SUR2A channel. Membrane potentials are indicated to the left of the traces. Dashed lines indicate the zero current level.

the core region (M1–H5–M2) of the Kir6.0 subunit since N- and C-termini have only a slight influence upon conductance (Kondo *et al.*, 1998). To determine which domain spanning this core region is responsible for the alteration in conductance properties, we constructed chimeras between the wild types of Kir6.2 (222) and Kir6.1 (111) as indicated in Figure 1A (left panel). Chimeras were prepared by replacing specific segments in the Kir6.2 core region, namely, the first transmembrane domain (M1), the second transmembrane domain (M2), the M1–H5 link (Lk1) or the H5–M2 link (Lk2), with the corresponding segments of the Kir6.1 channel. Exchange of the pore-forming domain (H5) between the Kir6.0 subtypes was unnecessary since the primary sequences are identical (Inagaki *et al.*, 1995a,b). We then measured the conductance of the different constructs co-expressed with SUR2A in HEK293T cells.

Replacement of either transmembrane domain M1 or M2 of 222 with that of 111 has little or no effect on channel conductance. As shown in Figure 1B (top left

panel), exchange of the M2 domain of 222 with that of 111, chimera 222(6.1M2), yielded larger single channel currents than chimera 212 which contained the whole Kir6.1 core region. Analysis by linear regression from a plot of unitary channel current amplitude against membrane potential (–100 to about –20 mV) of 222(6.1M2) revealed that its unitary conductance was 76.8 ± 2.3 pS (n = 5) which was not significantly different from that shown by 222 with 78 ± 0.2 pS (n = 5). Similarly, chimera 222(6.1M1) exhibited a large Kir6.2-like conductance of 71.3 ± 1.5 pS (n = 4). Therefore it was concluded that neither transmembrane segment contributes significantly to the conductance.

On the other hand, when the linker region between H5 and M2 of 222 was substituted with that of 111, chimera 222(6.1Lk2) showed a lower conductance of 63.2 ± 3.1 pS (n = 5), which was surprising as this construct differs from 222 by only one amino acid, namely, M148 in Kir6.1 versus V138 in Kir6.2. A reduced conductance of 52.3 ± 3.6 pS (n = 5) was also obtained from the 222(6.1Lk1) construct. As exchange of either of the extracellular links Lk1 or Lk2 caused only an intermediate reduction in single channel conductance, it was thought that transplanting the two links from 111 or 212 to 222 might have more effect. Figure 1B demonstrates that the unitary currents of chimera 222(6.1Lk1,Lk2) were smaller than those of chimera 222(6.1M2) and comparable with those of chimera 212 which contained the entire core region of Kir6.1. A plot of unitary current amplitude against membrane potential yielded a conductance of 43.3 ± 1.3 pS (n = 5) for the 222(6.1Lk1,Lk2) construct. This represents an ~2-fold reduction of the conductance shown by 222. These data suggest that the two extracellular links (Lk1 and Lk2) between the transmembrane segments and the H5 pore-forming region have important roles in determining the single channel conductance of Kir6.0 subunits.

Identification and evaluation of critical sites in the extracellular linker domains of Kir6.0 subunits

A close examination of the primary structure of Kir6.0 subunits in the extracellular linker domain (Figure 2A) reveals a highly divergent amino acid sequence at the M1–H5 side (Lk1) and a single amino acid change on the H5–M2 side (Lk2). To narrow down our choices, we segregated stretches of divergent amino acid residues and designated the cassette mutants as ‘a’, ‘b’, ‘c’ and ‘d’ in Lk1 and ‘e’ in Lk2. Each corresponding segment was swapped between chimeras 212 and 222 as shown in Figure 2B (left panel).

The Lk2 regions in Kir6.1 and Kir6.2 differ in only one amino acid residue, namely, M148 in Kir6.1 versus V138 in Kir6.2 and so this must be the residue critical for channel conductance in this segment. As shown in Figure 2B, substitution of V138 in Kir6.2 with M to produce chimera 222(6.1e) only causes a partial reduction in the channel conductance but one equivalent to having exchanged the entire H5–M2 link (Figure 1A). Since our aim was to construct a chimera of Kir6.2 with the conductance characteristics of Kir6.1, the search for the critical residues in Lk1 was conducted in chimeric Kir6.2 channels which already contained the ‘e’ region of Kir6.1, i.e. chimera 222(6.1e).

Although both chimeras 222(6.1ae) and 222(6.1be) contain insertions and substitutions of residues which would be likely to induce conformational adjustments in the channel structure, neither resulted in a channel of low conductance comparable with 212, though both had some effects (Figure 2B, right panel). The same applied for the construct 222(6.1de). However, when ‘c’ from Kir6.1 was transplanted to 222(6.1e) to form chimera 222(6.1ce), a conductance comparable with that of 212 was recorded (Figure 2B, right panel). The 222(6.1c) construct did not result in a conductance comparable with 222(6.1ce). Nor did it entirely correspond to the conductance of the chimera 222(Lk1) which contained the whole of the Kir6.1 M1–H5 link (Figure 1A). We cannot say therefore that the ‘c’ region accounts for the entire effect of the M1–H5 link upon single channel conductance but rather that simultaneously altering the ‘c’ and ‘e’ parts of 222 seemed to be conditional for obtaining a channel with the conductance properties of the Kir6.1 core region, chimera 212. In this case, the reciprocal experiment which replaces ‘c’ and ‘e’ in 212 with the corresponding sequences from Kir6.2 to give chimera 212(6.2ce) should result in a channel with the conductance properties of Kir6.2. Figure 2C shows single channel currents recorded from chimeras 222(6.1ce) and 212(6.2ce). Chimera 222(6.1ce) exhibited smaller single channel currents than those of 212(6.2ce) at any given membrane potentials. Analysis by linear regression yielded a unitary conductance of 42.7 ± 2.9 pS (n = 5) for 222(6.1ce) and 75.2 ± 2.5 pS (n = 5) for 212(6.2ce). We conclude that the critical sites responsible for the single channel conductance of Kir6.1 and Kir6.2 are the three amino acid residues that make up the region ‘c’ in the M1–H5 link and the single amino acid residue difference in the H5–M2 link.

The ‘c’ region of Kir6.2 consists of amino acid residues S113–I114–H115 while that of Kir6.1 consists of residues N123–V124–R125. We further dissected the ‘c’ region by replacing the Kir6.2 corresponding amino acid residues in the ‘c’ of 222(6.1e) with those from Kir6.1 (Figure 3, left panel). Among the constructs analyzed, we noticed that replacing S by N consistently yielded single channel conductances of $<$60 pS (Figure 3). The effect of replacement of H with R and/or I with V on channel conductance varied from one construct to another. Thus, S113 of Kir6.2 seems to have a particularly important role in determining the single channel conductance.

Modelling the Kir6.2 channel 3D structure

To derive a plausible mechanism for how the critical amino acid residues in Kir6.2 affect single channel conductance, we built a 3D structure model of Kir6.2 on the basis of the assumption that Kir6.0 subunits and the KcsA K^+ channel are structurally homologous (see Materials and methods for the construction of the tertiary model). We next mapped the positions of the critical residues determining the unitary conductance of Kir6.2 (Figure 4A and B) and also included the E–R residue pair that has been proposed to stabilize the pore loop of inwardly rectifying K^+ channels (Yang *et al.*, 1997). We also constructed the 3D structure model of 222(6.1ce) channel (Figure 4C).

The 3D structure model of Kir6.2 indicated that V138 faces the entrance of the pore. In the wild-type Kir6.2,

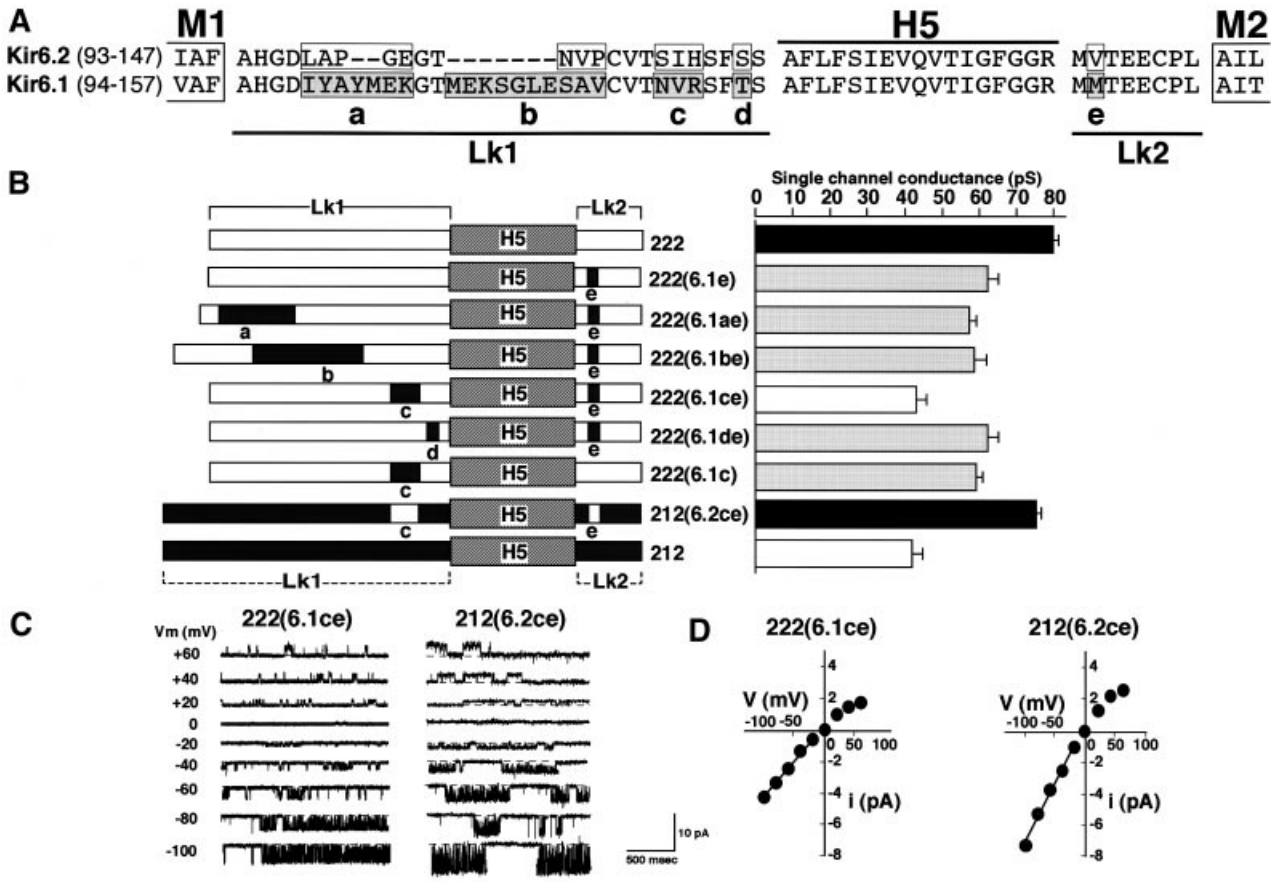

Fig. 2. Identification of critical sites within the extracellular links of Kir6.0 subunits. (**A**) Amino acid sequence alignment of the extracellular links Lk1 and Lk2, the pore-forming H5 and a part of the M1 and M2 transmembrane segments. Sections of divergent residues in the Lk1 and Lk2 regions of Kir6.1 and Kir6.2 are boxed and designated as 'a', 'b', 'c', 'd' and 'e'. (**B**) Chimeric constructs of the core region of Kir6.2 showing the relative position of the transplanted Kir6.1 segment in the host subunit (left panel) and their respective average unitary conductances obtained from five different patches for each mutant (right panel). In the left panel, Kir6.1 domains are shaded and the common H5 region is hatched. (**C**) Representative traces from single channel recording of chimeric Kir6.0/SUR2A channels. Left panel, the 222(6.1ce)/SUR2A channel. Right panel, the 212(6.2ce)/SUR2A channel. Membrane potentials are indicated to the left of the traces. Dashed lines indicate the zero current level. (**D**) Single channel current amplitude–voltage relationship of the chimeras in (C).

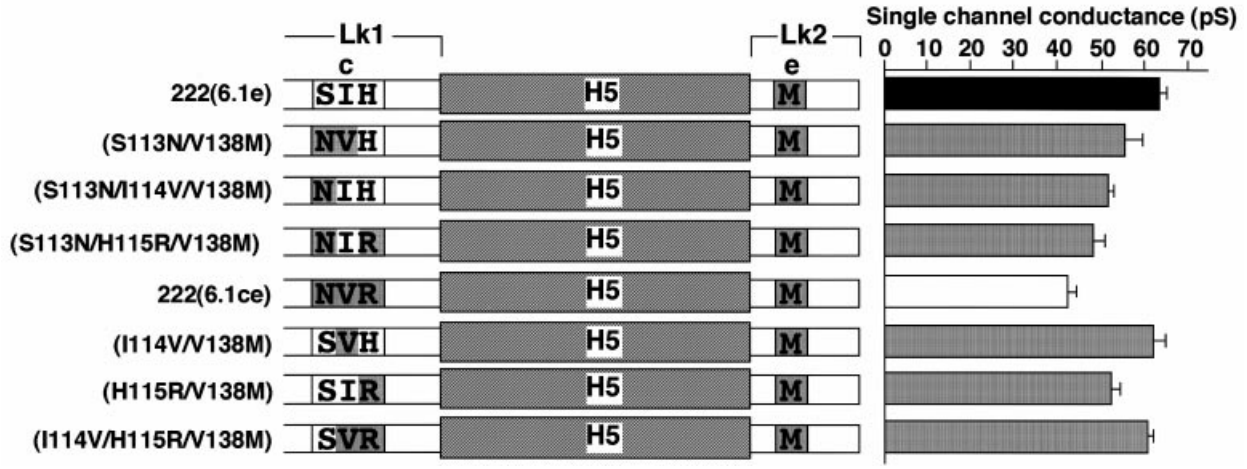

Fig. 3. Effects of specific amino acid residues in the critical 'c' region of the M1–H5 link on single channel conductance. Schematic diagram of mutant constructs of wild-type Kir6.2 showing amino acid substitutions in the extracellular linker domains (left panel) and their respective single channel conductance obtained from five different patches for each mutant (right panel). Amino acids are represented in single letter code and shaded if they represent residues found in the equivalent position in Kir6.1.

the diameter of the entrance surrounded by V138 in the tetramer was calculated as 10 Å (Figure 4B), while that surrounded by M138 in 222(6.1ce) was reduced to 5 Å (Figure 4C). We therefore tested the replacement of V at this site with other hydrophobic residues having different side-chain volume sizes. Substitution of V138 with L, M and F led to unitary conductances of 71.6 ± 2.3 pS (n = 4), 63.2 ± 3.1 pS (n = 5) and 60.3 ± 1.5 pS

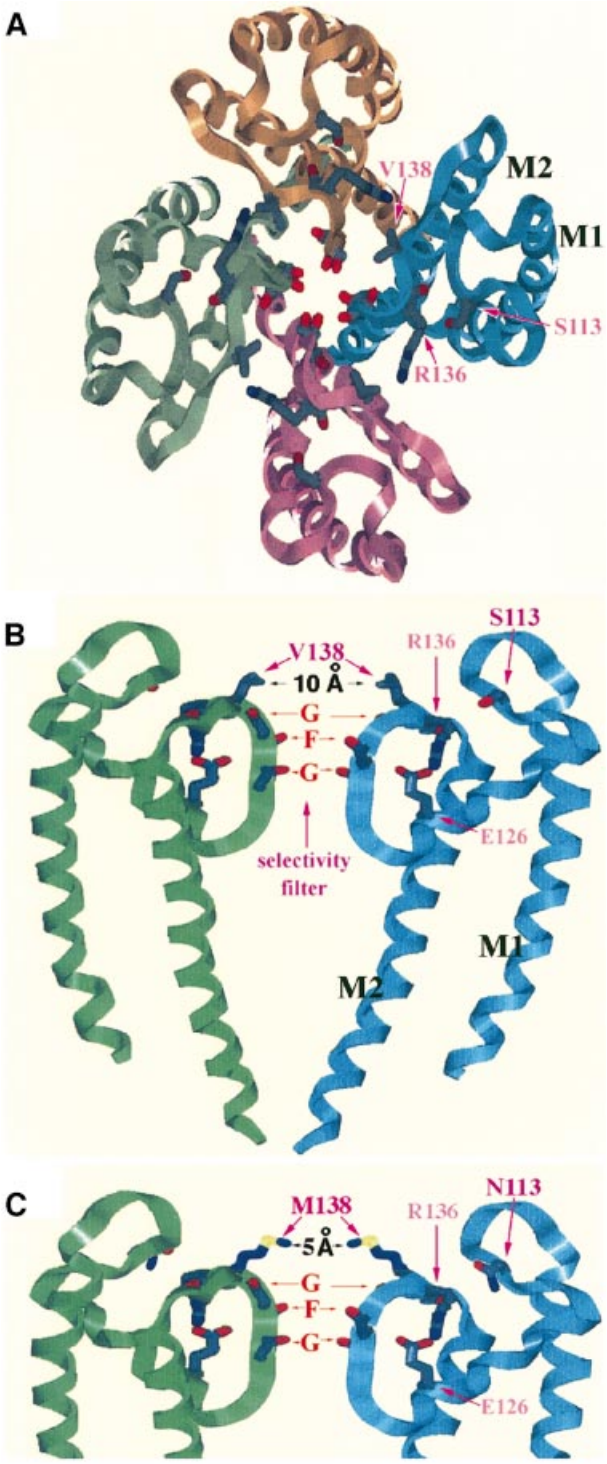

Fig. 4. Model of the 3D structure of Kir6.2. (**A**) Backbone structure of the channel pore viewed from the extracellular surface. (**B**) A perspective view of the channel, where the permeation pathway is oriented vertically with the extracellular surface up. Only two Kir6.2 subunits are shown. (**C**) The 222(6.1ce) channel from a perspective where the permeation pathway is oriented vertically with the extracellular surface up. Only two subunits are shown. Critical sites are labelled in A and B. Also included are the positions of the ion pair considered crucial in stabilizing the selectivity filter. They are E126 and R136, which correspond respectively to E138 and R148 in Kir2.1 (Yang *et al.*, 1997). The model is built based on the X-ray crystal structure of the KcsA K^+ channel (Doyle *et al.*, 1998; see Materials and methods).

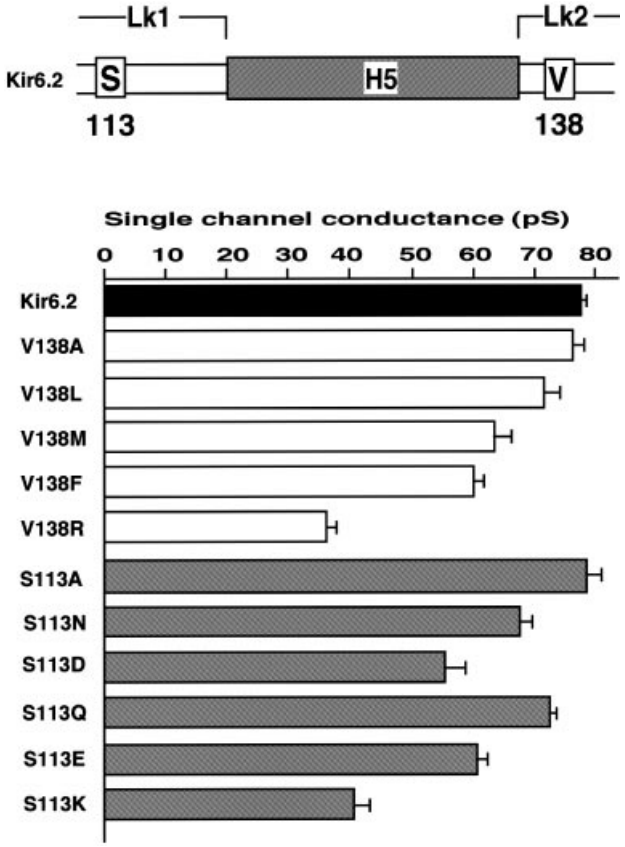

Fig. 5. Modulation of single channel conductance of Kir6.2 by mutations at critical sites 113 and 138. Amino acids are represented in single letter code. Numbers indicate the position of amino acid residues in the primary sequence of Kir6.2. Data were obtained from four or five different patches for each mutant.

(n = 4) (Figure 5), respectively, suggesting that side-chain volume might hinder the diffusion of K^+ ions. We further substituted V138 with R to examine the effect of positive charge at the position. In V138R, the unitary conductance was further reduced to 36.0 ± 1.5 pS (n = 4). This might be due to the repulsion of K^+ ions by the positive charge of R. This result may support our proposal that the amino acid residue at this site affects the diffusion of K^+ ions.

The model also suggests a putative hydrogen bond between S113 and R136 in Kir6.2. We therefore mutated Kir6.2S113 to A to verify whether the disruption of this putative hydrogen bond alters the single channel conductance. But as shown in Figure 5, the unitary conductance of Kir6.2S113A was 79 ± 2.5 pS (n = 4) which was not significantly different from that of the wild type. However, small decreases in conductance were noted for Kir6.2S113Q (72.8 ± 1.2 pS, n = 5), Kir6.2S113E (60.5 ± 0.8 pS, n = 4), Kir6.2S113N (67.2 ± 2.2, n = 4) and Kir6.2S113D (55.0 ± 3.0, n = 4). Of the mutations analyzed, Kir6.2S113K displayed the smallest unitary conductance with 41.4 ± 2.6 pS (n = 4).

Discussion

In this study we took advantage of the fact that two closely related members of a single ion channel subfamily present distinctly different ion permeabilities in order to

determine the molecular elements involved in controlling the rate of ion permeation through open channels. In this way we could avoid complications of interpretation resulting from mutational studies of any particular ion channel by focusing on attempting to provide the Kir6.2 channel with the conductance of Kir6.1 and vice versa. We found that the extracellular links between the transmembrane segments and the H5 pore region of the channels were critical determinants of the conductance difference. For the link between M1 and H5 three amino acid residues were critical, S113–I114–H115 in Kir6.2 and N123–V124–R125 in Kir6.1. For the link between H5 and M2 a single amino acid residue was critical, V138 in Kir6.2 and M148 in Kir6.1. Kir6.1 has nine extra amino acid residues in the M1–H5 link (Figure 2A). These amino acid residues seem to play no significant role in the permeation of K^+ ions through the Kir6.0/SUR channels, since 222(6.1ae) and 222(6.1be) channels possessed similar single channel conductance to 222(6.1e). Furthermore, the 212(6.2ce) channel exhibited the same conductance as the wild-type Kir6.2. Therefore, the c and e regions in the extracellular links may be almost fully responsible for the difference in the conductance between Kir6.1 and Kir6.2 channels. Both critical regions were required to express the respective conductance characteristics of Kir6.2 and Kir6.1, since chimeras expressing one region from each of Kir6.2 and Kir6.1 resulted in intermediate channel permeability.

Recently, Doyle *et al.* (1998) have determined the structure of a bacterial K^+ channel, KcsA, which has two transmembrane helices with the H5 region residing between them. Although the H5 region of KcsA is made up of amino acid residues which are most closely related to those of voltage-gated six-transmembrane eukaryotic K^+ channels (Schrempf *et al.*, 1995; Heginbotham *et al.*, 1997), it contains the K^+ channel signature sequence, G(Y/F)G, whose main chain carbonyl oxygen establishes the principles of K^+ selectivity. Therefore, K^+-selective channels may share structural similarity with KcsA, especially within the selectivity filter and the neighboring regions that are supposed to comprise part of the pore. This led us to use the available X-ray crystal structure of KcsA as the basis for a 3D structure model of Kir6.2 in order to integrate the information from our mutation studies and examine possible structural interactions that might control ion channel permeability (Figures 4 and 5).

An inspection of the Kir6.2 model reveals that Kir6.2V138 in the extracellular link between the H5 pore and the second transmembrane segment is positioned at the entrance of the pore mouth with its side chain exposed to the aqueous environment. It seemed possible that the amino acid residue occupying this site could directly influence the diffusion of permeant ions by steric interactions. This hypothesis was examined by exchanging the amino acid residue at site 138 of Kir6.2 for residues having different volumes or lengths of side chain. Our results show the single channel conductance of wild-type Kir6.2 = Kir6.2V138A > Kir6.2V138L > Kir6.2V138M > Kir6.2V138F (Figure 5), indicating that bulky residues resulted in reduced permeability. Actually, the model calculation indicated that the diameter of the entrance surrounded by the V138 in wild-type Kir6.2 was 10 Å but it was reduced to 5 Å in 222(6.1ce) (Figure 4B and C). These suggest that the amino acid at position 138 in the H5–M2 link of Kir6.2 influences ion channel conductance via steric hindrance effects by affecting the diffusion of K^+ ions. This notion may be supported by the observation that the positively charged residue at this site further reduced the permeability as shown in Kir6.2V138R (Figure 5). MacKinnon and Yellen (1990) have shown that substituting T449 in the H5–S6 linker region of the voltage-gated Shaker K^+ channel with K, R or Q resulted in a reduction of single channel conductance. Because T449 in the Shaker K^+ channel corresponds to V138 in Kir6.2, steric effects of the amino acid residues in the extracellular link between the selective filter and the subsequent transmembrane segment may be a general mechanism to control the quantity of ions permeating K^+ channels.

The spatial location of the triplet S113–I114–H115 in Kir6.2 is far from the channel entrance according to the 3D structure model (Figure 4). However, S113 is close to R136 which is considered to be crucial in maintaining the stability of the pore selectivity filter and which is highly conserved in inwardly rectifying K^+ channels (Yang *et al.*, 1997). It was therefore thought possible that site 113 in Kir6.2 affected single channel conductance by modifying the conformation of the permeation pathway via interaction with the critical residue R136. Our results, however, showed that a hydrogen bond interaction between the S113 side chain and R136 was not critical because the S113A mutant reproduced the single channel conductance of the wild type. When we replaced S113 with the neutral amino acid residues N and Q, which have larger side chains than A, the unitary conductance of the mutant channels was reduced. This suggests that the size of the amino acid residue at position 113 is important, since the side chain of S113 is close to and oriented towards the backbone of R136 in the model. Residues with larger side chains would make a steric clash and change the geometry around the crucial residue R136. In the cases of E and D, although their side-chain volumes are similar to those of Q and N, respectively, electrostatic interaction would further modify the disposition of R136 and therefore accounts for the difference in conductance between Kir6.2S113E and Kir6.2S113Q and also between Kir6.2S113D and Kir6.2S113N. When S113 was substituted with K, the single channel conductance was the smallest among various mutants at S113. Since K possesses a positive charge, it is likely that disposition of R136 can be caused by repulsion as well as attraction between the amino acid at 113 and R136. It seems, therefore, that site 113 and R136 in Kir6.2 are structurally correlated in order not only to maintain the stability of the pore selectivity filter as suggested by Yang *et al.* (1997), but also to fix the appropriate conformation of the permeation pathway depending on the side-chain volume and charge of the residue occupying position 113. Navaratnam *et al.* (1995) noted that Kir2.1 isolated from the cochlear sensory epithelium of the chick (cIRK1) exhibited a single channel conductance of 17 pS compared with 23 pS in its mouse counterpart (mIRK1). They attributed the difference to Q125 in cIRK1 and E at the corresponding site in mIRK1. This site corresponds to S113 in Kir6.2 and N123 in Kir6.1. This supports our contention that charged and uncharged residues positioned at this critical site establish distinct conformations of the permeation pathway owing

to the presence or absence of electrostatic interactions with the crucial residue R.

In Kir6.2, not only S113 but also the adjacent residues of I114 and H115 influence conductance (Figure 3). In the 3D structure model of Kir6.2, we could not identify specific factors associated with these residues that might influence the K^+ conduction pathway. It is probable that changes in the backbone conformation around S113–I114–H115 would occur from substitutions at these sites that would influence the interaction between the residue at site 113 and R136.

In the present study, we have identified structurally important amino acid residues in the extracellular links between transmembrane segments and the pore of Kir 6.0 subunits which account for the difference in the single channel conductance of Kir6.1/SUR2A and Kir6.2/SUR2A ion channels. By using a 3D structure model, we were able to elucidate specific factors at critical sites which contribute to the determination of the single channel conductance: (i) steric effects at Kir6.2V138 or Kir6.1M148 in the H5–M2 link which directly influence the diffusion of K^+; and (ii) structural constraints between Kir6.2S113 or Kir6.1N123 in the M1–H5 link and Kir6.2R136 or Kir6.1R146 which determine the conformation of the permeation pathway. These mechanisms highlight the importance of the spatial conformation of the channel particularly at the outer mouth of the pore. While a number of studies pinpoint the importance of the structure of the pore region in channel conductance along with its primary role in selectivity and functionality, there is also evidence that extra-pore domains affect channel conductance properties (Hartmann *et al.*, 1991; Lopez *et al.*, 1994; Taglialatela *et al.*, 1994). Thus, our findings may be applicable to other types of Kir channel.

Materials and methods

Molecular biology

All chimeric cDNAs and cassette mutants formed between Kir6.1 and Kir6.2, except for 212, were constructed using the GeneEditor™ *in vitro* site-directed mutagenesis system (Promega Corp., Madison, WI). Based on the alignment of Kir6.1 and Kir6.2 (Inagaki *et al.*, 1995a,b; Sakura *et al.*, 1995), the amino acid boundaries of the channel domains were defined (see Figure 1A) to design the desired chimeric constructs. Amino acid compositions formed between Kir6.1 and 6.2 of the various chimeras were as follows (numbers indicate Kir6.1 and Kir6.2 amino acid boundaries, respectively): 75–96 and 1–73 + 96–390, 222(6.1M1); 155–176 and 1–144 + 167–390, 222(6.1M2); 97–129 and 1–95 + 120–390, 222(6.1Lk1); 147–154 and 1–136 + 145–390, 222(6.1Lk2); 97–154 and 1–95 + 145–390, 222(6.1Lk1,Lk2). The 212 chimera was prepared according to the method described previously (Kondo *et al.*, 1998). To identify the critical sites in Lk1 of Kir6.1 or Kir6.2, stretches of divergent amino acid residues were segregated and labeled as cassette mutants 'a', 'b', 'c' and 'd'. Amino acid boundaries for 'a', 'b', 'c', 'd' and 'e' cassette mutants were 101–107, 110–119, 123–125, 128 and 148 of Kir6.1; 100–104, 107–109, 113–115, 118 and 138 of Kir6.2, respectively. Swappings of the corresponding cassette between that of Kir6.1 and Kir6.2 were made accordingly. All chimeras and cassette mutants constructed were confirmed by DNA sequencing.

Functional co-expression of SUR2A and Kir6.0/chimeric cDNAs

The coding regions of mouse SUR2A cDNA, and wild and chimeric cDNAs of Kir6.1 and Kir6.2 were subcloned into the expression vector, pcDNA3 (Invitrogen, San Diego, CA). These subcloned plasmids were transfected into human embryonic kidney (HEK) 293T cells using LipofectAMINE (Life Technology, Inc., Rockville, MD) according to the manufacturer's instructions. To monitor the efficiency of transfection, pCA-GFP (S65A) was also co-transfected. The cells expressing GFP were identified by fluorescence microscopy and used for electrophysiology.

Electrophysiology

The channels expressed in the co-transfected HEK293T cells were analyzed at the single-channel level by using the inside-out variant of the patch–clamp method with a commercially available patch–clamp amplifier (Axopatch 200A, Axon Instruments Inc., Foster City, CA). The bath was perfused with a solution containing (in mM): 150 KCl, 5 EGTA, 2 $MgCl_2$ and 5 HEPES–KOH (pH 7.3), in which the free Mg^{2+} concentration was 1.4 mM. The pipette solution contained (in mM): 150 KCl, 1 $MgCl_2$, 1 $CaCl_2$ and 5 HEPES–KOH (pH 7.4). The single channel currents were measured between –100 and +60 mV, and the single channel conductance was determined between –100 and –20 mV by using the linear regression method. All experiments were performed at room temperature (~25°C). The data were recorded on video cassette tapes using a PCM converter system (VR-10B, Instrutech Corp., New York, NY), and reproduced, low pass-filtered at 1 kHz (–3 dB) by an 8-pole Bessel filter (Frequency Devices, Haverhill, MA), sampled at 5 kHz and analyzed off-line on a computer (Macintosh Quadra 700, Apple Computer Inc., Cupertino, CA) using commercially available software (Patch Analyst Pro, MT Corporation, Nishinomiya, Hyogo, Japan). All data were derived from at least four distinct patches and expressed as mean values ±SD.

Construction of a tertiary model of Kir6.2

We constructed a tertiary model for Kir6.2 based on the X-ray crystal structure of KcsA K^+ channel (Doyle *et al.*, 1998) following the conventional method of homology modeling using a loop search method for the backbone structures (Nakamura *et al.*, 1991), a dead-end elimination method for the side-chain conformations (Tanimura *et al.*, 1994) and a conformation energy minimization for the structure refinement (Morikami *et al.*, 1992), using the AMBER force field (Weiner *et al.*, 1986).

Acknowledgements

We would like to thank Mari Imanishi and Akie Ito for technical assistance and Keiko Tsuji for secretarial support. This work is supported by grants from the Ministry of Education, Science, Sports and Culture of Japan, 'Research for the Future' Program of The Japan Society for the Promotion of Science (96L00302), and the Human Frontier Science Program (RG0158/1997-B).

References

Butler,A., Tsunoda,S., McCobb,D.P., Wei,A. and Salkoff,L. (1993) mSlo, a complex mouse gene encoding 'maxi' calcium-activated potassium channels. *Science*, **261**, 221–224.

Clement,J.P., Kunjilwar,K., Gonzalez,G., Schwanstecher,M., Panten,U., Aguilar-Bryan,L. and Bryan,J. (1997) Association and stoichiometry of K_{ATP} channel subunits. *Neuron*, **18**, 827–838.

Doyle,D.A., Cabral,J.M., Pfuetzner,R.A., Kuo,A., Gulbis,J.M., Cohen,S.L., Chait,B.T. and MacKinnon,R. (1998) The structure of the potassium channel: molecular basis of K^+ conduction and selectivity. *Science*, **280**, 69–77.

Hartmann,H.A., Kirsch,G.E., Drewe,J.A., Taglialatela,M., Joho,R.H. and Brown,A.M. (1991) Exchange of conduction pathways between two related K^+ channels. *Science*, **251**, 942–944.

Heginbotham,L., Odessey,E. and Miller,C. (1997) Tetrameric stoichiometry of a prokaryotic K^+ channel. *Biochemistry*, **36**, 10335–10342.

Inagaki,N., Gonoi,T., Clement,J.P., Namba,N., Inazawa,J., Gonzalez,G., Aguilar-Bryan,L., Seino,S. and Bryan,J. (1995a) Reconstitution of I_{KATP}: an inward rectifier subunit plus the sulfonylurea receptor. *Science*, **270**, 1166–1170.

Inagaki,N., Tsuura,Y., Namba,N., Masuda,K., Gonoi,T., Horie,M., Seino,Y., Mizuta,M. and Seino,S. (1995b) Cloning and functional characterization of a novel ATP-sensitive potassium channel ubiquitously expressed in rat tissues, including pancreatic islets, pituitary, skeletal muscle and heart. *J. Biol. Chem.*, **270**, 5691–5694.

Inagaki,N., Gonoi,T., Clement,J.P., Wang,C.-Z., Aguilar-Bryan,L., Bryan,J. and Seino,S. (1996) A family of sulfonylurea receptors determines the pharmacological properties of ATP-sensitive K^+ channels. *Neuron*, **16**, 1011–1017.

Isomoto,S., Kondo,C., Yamada,M., Matsumoto,S., Higashiguchi,O.,

Horio,Y., Matsuzawa,Y. and Kurachi,Y. (1996) A novel sulfonylurea receptor forms with BIR (Kir6.2) a smooth muscle type ATP-sensitive K^+ channel. *J. Biol. Chem.*, **271**, 24321–24324.

Jan,L.Y. and Jan,Y.N. (1997) Cloned potassium channels from eukaryotes and prokaryotes. *Annu. Rev. Neurosci*., **20**, 91–123.

Kondo,C., Repunte,V.P., Satoh,E., Yamada,M., Horio,Y., Matsuzawa,Y., Pott,L. and Kurachi,Y. (1998) Chimeras of Kir6.1 and Kir6.2 reveal structural elements involved in spontaneous opening and unitary conductance of the ATP-sensitive K^+ channels. *Receptors Channels*, **6**, 129–140.

Krapivinsky,G., Medina,I., Eng,L., Krapivinsky,L., Yang,Y. and Clapham,D.E. (1998) A novel inward rectifier K^+ channel with unique pore properties. *Neuron*, **20**, 995–1005.

Lopez,G.A., Jan,Y.N. and Jan,L.Y. (1994) Evidence that the S6 segment of the *Shaker* voltage-gated K^+ channel comprises part of the pore. *Nature*, **367**, 179–182.

MacKinnon,R. and Yellen,G. (1990) Mutations affecting TEA blockade and ion permeation in voltage-activated K^+ channels. *Science*, **250**, 276–279.

Morikami,K., Nakai,T., Kidera,A., Saito,M. and Nakamura,H. (1992) PRESTO: A vectorized molecular mechanics program for biopolymers. *Comput. Chem*., **16**, 243–248.

Nakamura,H., Katayanagi,K., Morikawa,K. and Ikehara,M. (1991) Structural models of ribonuclease H domains in reverse transcriptases from retro-viruses. *Nucleic Acids Res*., **19**, 1817–1823.

Navaratnam,D.S., Escobar,L., Covarrubias,M. and Oberholtzer,J.C. (1995) Permeation properties and differential expression across the auditory receptor epithelium of an inward rectifier K^+ channel cloned from the chick inner ear. *J. Biol. Chem.*, **270**, 19238–19245.

Sakura,H., Ämmälä,C., Smith,P.A., Gribble,F.M. and Aschcroft,F.M. (1995) Cloning and functional expression of the cDNA encoding a novel ATP-sensitive potassium channel subunit expressed in pancreatic β-cells, heart and skeletal muscle. *FEBS Lett.*, **377**, 338–344.

Satoh,E., Yamada,M., Kondo,C., Repunte,V.P., Horio,Y., Iijima,T. and Kurachi,Y. (1998) Intracellular nucleotide-mediated gating of SUR/Kir6.0 complex potassium channels expressed in a mammalian cell line and its modification by pinacidil. *J. Physiol.*, **511**, 663–674.

Schrempf,H., Schmidt,O., Kummerlen,R., Hinnah,S., Muller,D., Betzler,M., Steinkamp,T. and Wagner,R. (1995) A prokaryotic potassium ion channel with two predicted transmembrane segments from *Streptomyces lividans*. *EMBO J.*, **14**, 5170–5178.

Shyng,S. and Nichols,C.G. (1997) Octameric stoichiometry of the K_{ATP} channel complex. *J. Gen. Physiol*., **110**, 655–664.

Taglialatela,M., Champagne,M.S., Drewe,J.A. and Brown,A.M. (1994) Comparison of H5, S6 and H5-S6 exchanges on pore properties of voltage-dependent K^+ channels. *J. Biol. Chem*., **269**, 13867–13873.

Tanimura,R., Kidera,A. and Nakamura,H. (1994) Determination of protein side-chain packing. *Protein Sci.*, **2**, 2358–2365.

Yamada,M., Isomoto,S., Matsumoto,S., Kondo,C., Shindo,T., Horio,Y. and Kurachi,Y. (1997) Sulphonylurea receptor 2B and Kir6.1 form a sulphonylurea-sensitive but ATP-insensitive K^+ channel. *J. Physiol. Lond.*, **499**, 715–720.

Yang,J., Yu,M., Jan,Y.N. and Jan,L.Y. (1997) Stabilization of ion selectivity filter by pore loop ion pairs in an inwardly rectifying potassium channel. *Proc. Natl Acad. Sci. USA*, **94**, 1568–1572.

Weiner,S.J., Kollman,P.A., Nguyen,D.T. and Case,D. (1986) An all atom force field for simulation of proteins and nucleic acids. *J. Comput. Chem*., **7**, 230–252.

Received January 25, 1999; revised and accepted April 20, 1999